

Characterization of the local density-of-states fluctuations near the integer quantum Hall transition in a quantum-dot array

Giancarlo Jug*

Max-Planck-Institut für Physik Komplexer Systeme, Außenstelle Stuttgart, Postfach 800665, D-70569 Stuttgart, Germany

Klaus Ziegler

Max-Planck-Institut für Physik Komplexer Systeme, Außenstelle Stuttgart, Postfach 800665, D-70569 Stuttgart, Germany
and Institut für Physik, Universität Augsburg, D-86135 Augsburg, Germany

(Received 26 December 1996)

We present a calculation for the second moment of the local density of states in a model of a two-dimensional quantum dot array near the quantum Hall transition. The quantum dot array model is a realistic adaptation of the lattice model for the quantum Hall transition in the two-dimensional electron gas in an external magnetic field proposed by Ludwig, Fisher, Shankar, and Grinstein. We make use of a Dirac fermion representation for the Green's functions in the presence of fluctuations for the quantum dot energy levels. A saddle-point approximation yields nonperturbative results for the first and second moments of the local density of states, showing interesting fluctuation behavior near the quantum Hall transition. To our knowledge we discuss here one of the first analytic characterizations of chaotic behavior for a two-dimensional mesoscopic structure. The connection with possible experimental investigations of the local density of states in the quantum dot array structures (by means of NMR Knight-shift or single-electron-tunneling techniques) and our work is also established. [S0163-1829(97)02736-7]

I. INTRODUCTION

Recently, there has been a considerable surge of interest in the electronic properties of nanometric-scale metal and semiconductor structures.^{1,2} Static as well as transport properties of these systems can be obtained from the knowledge of the statistics of the energy level distribution for quantum-mechanical structures in which weak disorder (or quantum chaos) plays a fundamental role. The presence of an external magnetic field enhances the influence of the quantum fluctuations on the properties of these mesoscopic systems. The remarkable advances in nanostructure fabrication procedures have also lead recently to a good deal of experimental and theoretical studies of the properties of quantum dots, quantum wires and, moreover, of quantum dot arrays³ (QDA) which can be obtained by a variety of techniques at semiconductor surfaces and interfaces. All these mesoscopic structures exhibit a wealth of new interesting quantum phenomena in an external magnetic field and at low temperatures. In particular, QDA (as "artificial crystals") offer the possibility of investigating situations not accessible in natural crystals for the magnetic fields that can be produced in normal laboratory conditions.

On the other hand, a most celebrated quantum phenomenon, occurring at low temperatures in the presence of a magnetic field and assisted by the presence of weak disorder in a two-dimensional (2D) semiconductor heterostructure, is the integer quantum Hall effect (IQHE).⁴ The plateaus in the Hall conductivity are believed to be the result of current-carrying edge states and localized bulk states.⁵ The transitions between plateaus are due to localization-delocalization transitions induced by the combined effects of the magnetic field and disorder close to zero absolute temperature.⁶ The behavior near a single IQHE transition (QHT) can be described in a number of ways, theoretically, in order to repro-

duce the jump in the conductivity and other singularities near the QHT. A model for the IQHE that is particularly suited to the present work has been proposed and studied by Ludwig *et al.*⁷ In this model, a square lattice hopping model is defined, with a fixed half-flux-quantum $\frac{1}{2}\Phi_0$ per plaquette defining the lattice spacing a , with both nearest-neighbor and next-nearest-neighbor hopping processes considered in the presence of a staggered chemical potential and suitable forms of the one-particle disordered potential. In the continuum limit, $a \rightarrow 0$ formally, and near the QHT this model yields a valid description of the behavior near a single IQHE step.^{7,8}

It would seem natural, therefore, to extend the model of Ludwig *et al.* to the description of the QHT in a QDA system. This has indeed been done,⁹ by taking into account the fluctuations of the quantum levels pertinent to a single quantum dot. The existence of a supporting lattice in the QDA also makes the model of Ludwig *et al.*, as extended and studied by Ziegler,⁹ physically more appealing. In this model a QHT is indeed found and described in the proximity of the transition point. It is found that the otherwise sharp QHT step becomes rounded by the presence of level fluctuations in the single dots.

In this paper we present an analytical characterization of the fluctuations of the local density of states (DOS) for a QDA near the QHT, using the model and calculations presented in Ref. 9. Our calculation is interesting in its own right for a good number of reasons. First and foremost, the averaged DOS and the moments of its distribution due to level statistics can be studied by means of Knight shift NMR measurements, now becoming accessible for semiconductor heterostructures.¹⁰ Another candidate technique for measuring local DOS-related properties is the single-electron tunneling (SET),¹¹ which provides an imaging of the local DOS in (bulk) semiconductors. A more detailed discussion will be presented in the Conclusions, Sec. IV. Also, from the more

theoretical point of view, it is of interest to characterize the fluctuations near the QHT of an observable quantity like the DOS, considering that in the absence of fluctuations in the levels of a dot the DOS itself vanishes at the center of the band, $E=0$. When fluctuations are present, a semicircle law is obtained for the averaged local DOS $\langle \rho(\mathbf{r}) \rangle$ which does not vanish anymore at $E=0$. The second moment of the global DOS vanishes identically, but not that of the local DOS

$$M_2(m) = \langle \rho(\mathbf{r}, m)^2 \rangle - \langle \rho(\mathbf{r}, m) \rangle^2, \quad (1)$$

which we calculate in this work. Here, m plays the role of a chemical potential which controls the density of fermions in the system (for details see Sec. II). We find that M_2 diverges near the point $m=m_c$ where $\langle \rho(\mathbf{r}, m) \rangle$ vanishes, indicating that the level fluctuations are particularly strong near this value of the energy. From the technical point of view, our work represents an attempt to characterize quantum mesoscopic fluctuations in a system of dimensionality $D>1$ without applying the $2+\epsilon$ expansion technique. Most approximate methods in fact deal with $D=0$ systems in the end (e.g., single dots, or aggregates of small metallic particles) and more rigorous and/or numerical work has been done chiefly for one-dimensional systems. An alternative approach to random electronic systems remains, naturally, the above-mentioned $2+\epsilon$ expansion technique,^{12,13} which however applies only to the scaling regime near the mobility edge. Therefore, our contribution to this field is instrumental for extending theoretical research to systems of dimensionality $D=2$, as our calculations can indeed be implemented, with some additional computational effort, for the characterization of the higher moments of the local DOS, as well as of those for the conductivity. As a further remark, we point out that the straight quantum Hall system can be viewed as a mesoscopic-like system itself in terms of the recently discovered¹⁴ universal conductance fluctuations between quantum Hall plateaus near the QHT. This indicates, as confirmed by very recent numerical studies,^{15,16} that the characterization of the electronic states in the presence of level fluctuations for 2D electron-gas systems is of interest even before the complications of a periodic QDA structure are inserted in these devices.

The paper is organized as follows. In Sec. II we define the details of the model and justify its applicability to the QDA system in the close proximity of the QHT. This is a model for quasiparticles (quasielectrons) in a lattice of "artificial atoms" (the QDA); the quasiparticle levels are subject to some statistics with strong correlations of universal nature and characterized by a Wigner-Dyson distribution.^{17,18} The model is set up with a fixed flux $\frac{1}{2}\Phi_0$ per plaquette, but although this may imply a fixed value of the magnetic field, we stress that the presence of a (staggered) chemical potential μ allows one to tune the model in the close vicinity of a QHT. The model includes a random potential, and we take the point of view that a random (Dirac) mass for the electrons is adequate in capturing the physics of the level fluctuations inside a single quantum dot. In Sec. III we briefly discuss the functional integral representation for the appropriate products of Green's functions, following standard procedures.^{19,20} We set up a representation in terms of super-

fields (bosonic as well as fermionic) to take care of the averaging over level fluctuations, and carry out a large- N saddle-point approximation to evaluate the first and second moments of the local DOS near the QHT. This is a justified approximation when $N \approx 10^2$ represents the number of single quantum dot levels, but the case $N=1$, representing the straight quantum Hall system, can in principle also be described by this approximation. We carry out the analysis for the Gaussian fluctuations and present our results. These are discussed in the conclusions, Sec. IV, where the connection with some other recent papers on the subject is established, as is the connection between our results and their possible experimental verification by means of NMR Knight shift or SET measurements.

II. THE MODEL

A 2D array of quantum dots in a homogeneous perpendicular magnetic field can be modeled by a tight-binding tunneling (or hopping) Hamiltonian which, neglecting quasiparticle interactions, takes the quadratic form $\mathcal{H} = \sum_r H_{r,r'}^{\alpha,\alpha'} c_r^{\alpha^2} c_{r'}^{\alpha'} + \text{H.c.}$, with $c_r^{\alpha^2}$ creating a quasielectron at QDA site r in single-dot level $\alpha=1,2,\dots,N$. The matrix elements $H_{r,r'}^{\alpha,\alpha'}$ are chosen as⁹

$$H_{r,r'}^{\alpha,\alpha'} = H_r^{(0)\alpha,\alpha'} \delta_{r,r'} + H_{r,r'}^{(t)} \delta_{\alpha,\alpha'} + V_r \delta_{r,r'} \delta_{\alpha,\alpha'}. \quad (2)$$

Here we take the point of view that the single-dot electronic states are statistically distributed with matrix elements $H_r^{(0)\alpha,\alpha'}$ defined by the Gaussian unitary ensemble statistics: $\langle H_r^{(0)\alpha,\alpha'} H_r^{(0)\beta,\beta'} \rangle = (g/N) \delta_{\alpha,\beta} \delta_{\alpha',\beta'}$, g being the strength of the level fluctuations depending on the nature of the interactions and/or disorder and chaos inside a single dot. We take, at least initially, the point of view that weak tunneling processes take place between neighboring dots and within the same single-dot energy levels. Strictly speaking our formulation already contains tunneling between different neighboring dots' energy levels via the random occupation of levels pertinent to each individual dot. Here, tunneling diagonal in the level indices will be assumed as realistic for the actual calculations and we take the tunneling rates to be nonvanishing only between nearest-neighboring and next-nearest-neighboring dots. These rates take into account the presence of a magnetic field that can be thought of as fixed at the value $B = \Phi_0/2a^2$, in correspondence with the spacing a (typically³ one has $a = 100 \pm 500$ nm) between the dots. In the Landau gauge, the tunneling Hamiltonian matrix elements read [setting $\mathbf{r} = (x, y)$ and indicating with e_x and e_y the lattice unit vectors]

$$H_{r,r'}^{(t)} = t e^{\pi i y/a} \delta_{r',r+e_x} + t \delta_{r',r+e_y} \pm i t' e^{\pi i y/a} \delta_{r',r+e_x \pm e_y} + \text{H.c.} \quad (3)$$

Finally, the potential V_r represents an additional (e.g., electric) external field and can be regarded as a staggered chemical potential: $V_r = (-1)^{x+y} \mu$, which opens a gap 2μ in the spectrum of the quasielectrons. For the "simple" IQHE situation, the model reduces to its $N=1$ limit and corresponds to the model proposed for the QHT by Ludwig *et al.*⁷ We as-

sume for the QDA that the separation a between the dots is much greater than the dots' size.

Now, following a standard procedure,^{7,8} the model (2) is reduced in the continuum limit (formally $a \rightarrow 0$) and for long wavelengths to an equivalent 2D Dirac Hamiltonian^{8,9}

$$H^{\alpha\beta} = i(\sigma_1 \nabla_1 + \sigma_2 \nabla_2) \delta_{\alpha,\beta} + \sigma_3 M^{\alpha\beta} \quad (\alpha, \beta = 1, \dots, N). \quad (4)$$

∇ is here the 2D (lattice) gradient operator, σ_j are Pauli matrices, and M is a random mass matrix with mean $m \equiv \mu - t'$: $M_r^{\alpha\beta} = m \delta_{\alpha,\beta} + \delta M_r^{\alpha\beta}$ with $\langle \delta M_r^{\alpha\beta} \delta M_{r'}^{\alpha'\beta'} \rangle_{\delta M} = (g/N) \delta_{\alpha,\beta'} \delta_{\alpha',\beta} \delta_{r,r'}$. The tunneling rate t is scaled out in the Hamiltonian. Therefore, m is measured in units of t and the fluctuation parameter g is measured in units of t^2 . This model, for $N=1$ and within a saddle-point approximation, describes the jump in the conductivity characterizing the QHT and displays for the local DOS a characteristic semicircle law.^{8,20} The transition is driven either by changing the external field or, equivalently, as will be argued in this work, by changing the chemical potential μ .

In principle there can be three different types of randomness: a random Dirac mass, a random energy, and a random vector potential. We believe, however, that the random mass alone correctly accounts for the effects of the level fluctuations in the single quantum dots. The random vector potential does not break the time reversal symmetry of the massless Dirac fermions. This is a strong restriction which implies that the case of the massless model has very special properties.⁷ Most remarkable is the fact that the average DOS is singular and obeys a power law: $\langle \rho(E) \rangle \sim E^\alpha$ with $-1 < \alpha < 1$. This is an unphysical behavior because the DOS should be finite at the Hall transition. A finite DOS exists for a random Dirac mass^{9,20} and for a random energy term.²¹ [Ludwig *et al.*⁷ obtained for a random Dirac mass the result of a vanishing DOS at the Hall transition, using a perturbative renormalization group calculation. Consequently, they argued that only a combination of a random mass and a random vector potential can lead to a nonzero DOS. However, a nonperturbative approach gives a nonzero DOS already for a random Dirac mass,⁹ proportional to $\exp(-\pi/g)$.] The random Dirac mass creates spontaneously a contribution proportional to the random energy (see Ref. 9 and Sec. III A of this paper). This implies that including the random energy will not lead to a qualitative change of the effect of the random Dirac mass.

Results from previous calculations with this model will be recalled below; here it suffices to notice that the Green's function $G = (H + i\epsilon\sigma_0)^{-1}$ has special properties because of the Lorentz invariance of the Dirac theory. In particular we will make use in the following of the relation $(G_{11,rr}^{\alpha\alpha})^* = -G_{22,rr}^{\alpha\alpha}$. Here, and in the following, σ_0 is a convenient notation²² for the 2×2 unit matrix.

As a last remark about the model, we now clarify the role of the "fixed" magnetic flux per plaquette. The physical parameter of the model is not the magnetic flux, but the filling factor $\nu = n\Phi_0/B$ (n is here the density of particles, B the external magnetic field). n can be written as the total number of particles divided by the total area of the system. Since the particles are noninteracting fermions, there are at most N particles, if N is the number of lattice sites. The local

DOS is symmetric around $E=0$. This implies that there are $N/2$ particles at $E=0$. On the other hand, the lattice can be divided into plaquettes of four lattice sites each. The flux through each plaquette is $\Phi_0/2 = a^2 B$, if a^2 is the area of the plaquette. Taking into account that there are N plaquettes (in the thermodynamic limit, when boundary effects can be ignored), we can write for the filling factor

$$\nu = (N/2)\Phi_0/(Na^2B) = (N/2)\Phi_0/(N\Phi_0/2) = 1. \quad (5)$$

Hence, the filling factor is 1, regardless of all other model parameters.

A. Second moment of the local DOS

According to standard Green's function theory, the local DOS (LDOS) is obtained from

$$\begin{aligned} \rho^{\alpha\alpha}(r, M) &= \frac{1}{\pi} \text{Im} [G_{11,rr}^{\alpha\alpha} + G_{22,rr}^{\alpha\alpha}] \\ &= \frac{i}{2\pi} [G_{11,rr}^{\alpha\alpha} + G_{22,rr}^{\alpha\alpha} - (G_{11,rr}^{\alpha\alpha})^* - (G_{22,rr}^{\alpha\alpha})^*]. \end{aligned} \quad (6)$$

For the tight-binding model without magnetic field this implies that one has to evaluate the two-particle Green's function with opposite signs of the frequency (advanced and retarded Green's functions) in order to get the second moment of the LDOS.^{19,28} This is the same problem as in the evaluation of the conductivity. In the model with half a flux quantum per plaquette, however, we can use the relation $(G_{11,rr}^{\alpha\alpha})^* = -G_{22,rr}^{\alpha\alpha}$ to write

$$\rho^{\alpha\alpha}(r, M) = \frac{i}{\pi} (G_{11,rr}^{\alpha\alpha} + G_{22,rr}^{\alpha\alpha}), \quad (7)$$

and consequently

$$\begin{aligned} \rho^{\alpha\alpha}(r, M) \rho^{\beta\beta}(r, M) &= -\frac{1}{\pi^2} (G_{11,rr}^{\alpha\alpha} + G_{22,rr}^{\alpha\alpha})(G_{11,rr}^{\beta\beta} + G_{22,rr}^{\beta\beta}). \end{aligned} \quad (8)$$

In this way we set out to evaluate

$$\begin{aligned} M_2^{\alpha\beta} &= \langle \rho^{\alpha\alpha}(r, M) \rho^{\beta\beta}(r, M) \rangle_{\delta M} \\ &\quad - \langle \rho^{\alpha\alpha}(r, M) \rangle_{\delta M} \langle \rho^{\beta\beta}(r, M) \rangle_{\delta M} \\ &= -\frac{1}{\pi^2} (\langle G_{11,rr}^{\alpha\alpha} G_{11,rr}^{\beta\beta} \rangle_{\delta M} - \langle G_{11,rr}^{\alpha\alpha} \rangle_{\delta M} \langle G_{11,rr}^{\beta\beta} \rangle_{\delta M} \\ &\quad + \langle G_{11,rr}^{\alpha\alpha} G_{22,rr}^{\beta\beta} \rangle_{\delta M} - \langle G_{11,rr}^{\alpha\alpha} \rangle_{\delta M} \langle G_{22,rr}^{\beta\beta} \rangle_{\delta M}) + [1 \leftrightarrow 2]. \end{aligned} \quad (9)$$

III. FUNCTIONAL INTEGRAL REPRESENTATION

By means of a standard representation, we write, quite generally²⁰

$$\begin{aligned} G_{rr,jj}^{\alpha\alpha} &= -i \int \chi_{r,j}^{\alpha} \chi_{r,j}^{\alpha} \exp(-S_1) \prod_r d\Phi_r d\bar{\Phi}_r \\ &\equiv -i \langle \chi_{r,j}^{\alpha} \chi_{r,j}^{\alpha} \rangle_S, \end{aligned} \quad (10)$$

and consequently

$$G_{rr,jj}^{\alpha\alpha} G_{rr,kk}^{\beta\beta} = \int \chi_{r,j}^\alpha \chi_{r,j}^\beta \Psi_{r,k}^\alpha \Psi_{r,k}^\beta \exp(-S_1) \prod_r d\Phi_r d\bar{\Phi}_r \equiv \langle \chi_{r,j}^\alpha \chi_{r,j}^\beta \Psi_{r,k}^\alpha \Psi_{r,k}^\beta \rangle_S, \quad (11)$$

with the supersymmetric action (sum convention for α)

$$S_1 = -i\sigma_\epsilon \left[\Phi, (H_0 + \epsilon\sigma_0) \bar{\Phi} \right] + \sum_r \delta M_r^{\alpha\alpha'} (\Phi_r^{\alpha'} \cdot \sigma_3 \bar{\Phi}_r^\alpha), \quad (12)$$

where $\sigma_\epsilon = \text{sign}(\epsilon)$ and the \mathbb{R} eld $\Phi_{r,j}^\alpha = (\Psi_{r,j}^\alpha, \chi_{r,j}^\alpha)$. The \mathbb{R} st component is Grassmann and the second complex. We notice that the normalization of the functional integral in Eq. (11) is due to the combination of Grassmann and complex \mathbb{R} elds. Averaging with Gaussian distributed $\bar{\text{uctuations}}$ in the "masses" $M_r^{\alpha\beta}$ yields $\exp(-S_2) = \langle \exp(-S_1) \rangle_{\delta M}$, with

$$S_2 = -i\sigma_\epsilon \left[\Phi, (H_0 + \epsilon\sigma_0) \bar{\Phi} \right] + \frac{g}{N} \sum_r (\Phi_r^\alpha \cdot \sigma_3 \bar{\Phi}_r^\alpha)^2. \quad (13)$$

Thus we have derived an effective \mathbb{R} eld theory for Φ which serves as a generating functional for the averaged Green's function. It is important to notice that *not only* δM creates the fermion-fermion interaction in Eq. (13) but that also other types of randomness can do this job. For instance, the interaction can also be created by a term which couples to a matrix \mathbb{R} eld ($\mu = 1, \dots, 4$ includes the complex and Grassmann components):

$$\exp \left[-\frac{g}{N} \sum_r (\Phi_r^\alpha \cdot \sigma_3 \bar{\Phi}_r^\alpha)^2 \right] = \int \exp \left[-(N/g) \sum \tilde{\mathcal{Q}}_{r;\mu,\mu'}(\sigma_3)_{\mu'} \tilde{\mathcal{Q}}_{r;\mu',\mu}(\sigma_3)_\mu - i \sum \tilde{\mathcal{Q}}_{r;\mu,\mu'} \Phi_{r,\mu}^\alpha \bar{\Phi}_{r,\mu}^\alpha \right] \mathcal{D}[\tilde{\mathcal{Q}}], \quad (14)$$

with the supermatrix

$$S_3 = \frac{1}{g} \text{Trg} \begin{pmatrix} Q & \bar{\Phi} \\ \Theta & -iP \end{pmatrix} + \ln \left[\detg \begin{pmatrix} i(H_1 + i\epsilon\sigma_0 - 2\tau Q\tau) & -2i\tau\bar{\Phi} \\ -2i\tau\Theta\tau & i(H_1 + i\epsilon\sigma_0 + 2i\tau P\tau) \end{pmatrix} \right], \quad (19)$$

where we have introduced the graded (or¹⁹ super-) trace and determinant. This implies for the local DOS

$$\frac{1}{N} \sum_\alpha \langle \rho^{\alpha\alpha}(r, M) \rangle_{\delta M} = \frac{1}{N\pi} \sum_\alpha \sum_j \langle \chi_{r,j}^\alpha \chi_{r,j}^\alpha \rangle_S = \frac{i}{g\pi} \sum_j \langle [\tau Q_r \tau]_{jj} \rangle_Q. \quad (20)$$

For the correlation of the local DOS, it follows that

$$\tilde{\mathcal{Q}} = \begin{pmatrix} Q & \bar{\Phi} \\ \Theta & -iP \end{pmatrix}. \quad (15)$$

The \mathbb{R} eld Φ appears only in a quadratic form on the right-hand side. Therefore, it can be integrated out. This leads to

$$\langle G_{rr,jj}^{\alpha\alpha} \rangle_{\delta M} = \int \mathcal{G}_{11,jj} \exp(-NS_3) \mathcal{D}[Q, P, \Theta] \equiv \langle \mathcal{G}_{11,jj} \rangle_Q, \quad (16)$$

and consequently

$$\begin{aligned} \langle G_{rr,jj}^{\alpha\alpha} G_{rr,kk}^{\beta\beta} \rangle_{\delta M} &= \int (-\mathcal{G}_{12,kj} \mathcal{G}_{21,jk} \delta_{\alpha,\beta} + \mathcal{G}_{11,jj} \mathcal{G}_{22,kk}) \\ &\quad \times \exp(-NS_3) \mathcal{D}[Q, P, \Theta] \\ &\equiv \langle -\mathcal{G}_{12,kj} \mathcal{G}_{21,jk} \delta_{\alpha,\beta} + \mathcal{G}_{11,jj} \mathcal{G}_{22,kk} \rangle_Q, \end{aligned} \quad (17)$$

where we have defined

$$\mathcal{G} = \begin{pmatrix} G_0^{-1} - 2\tau Q\tau & -2\tau\bar{\Phi} \\ -2\tau\Theta\tau & G_0^{-1} + 2i\tau P\tau \end{pmatrix}_{rr}^{-1}. \quad (18)$$

Here $G_0 = (H_0 + i\epsilon\sigma_0)^{-1}$, $\tau = \sqrt{\sigma_3}$, $H_0 \equiv \langle H \rangle = (\sigma_1 \nabla_1 + \sigma_2 \nabla_2) + \sigma_3 m$, and

$$\begin{aligned} M_2^{\alpha\beta} &= \frac{1}{\pi^2} \sum_{j,k=1}^2 [\langle \mathcal{G}_{12,kj} \mathcal{G}_{21,jk} \delta_{\alpha,\beta} - \mathcal{G}_{11,jj} \mathcal{G}_{22,kk} \rangle_Q \\ &\quad + \langle \mathcal{G}_{11,jj} \rangle_Q \langle \mathcal{G}_{11,kk} \rangle_Q]. \end{aligned} \quad (21)$$

A. Saddle-point approximation

The number of levels N appears in front of the action. Thus the effect of level $\bar{\text{uctuations}}$ for $N \rightarrow \infty$ can be evaluated within a saddle-point approximation (SPA).²⁰ The SP equation reads

$$\frac{\delta}{\delta Q} \left[\frac{1}{g} \text{Tr} Q^2 + \text{ln det}(G_0^{-1} - 2\tau Q \tau) \right] = 0. \quad (22)$$

A second SP equation appears from the variation of P by replacing $Q \rightarrow -iP$. As an ansatz we take a uniform SP solution $Q_0 = -iP_0 = -(1/2)[i\eta\sigma_3 + m_s\sigma_0]$. Then Eq. (22) leads to the conditions $\eta = \eta g I$, $m_s = -mgI/(1+gI)$ with the integral $I = \int [(m+m_s)^2 + \eta^2 + k^2]^{-1} d^2k/2\pi^2$. There is both a trivial and a nontrivial solution, $\eta = 0$ and $\eta \neq 0$. The latter is possible for $m^2 < m_c^2$ with $m_c = 2\exp(-\pi/g)$. This means the level fluctuations shift the energy $\epsilon \rightarrow \epsilon + \eta$ and the Dirac mass $m \rightarrow m + m_s$, where $\eta(m)$ and $m_s(m)$ are solutions of the SP equation (22). The sign of η is fixed by the condition that η must be analytic in ϵ ; this leads to $\text{sign}(\eta) = \text{sign}(\epsilon)$. It is important to notice that η is proportional to the energy and *not* to the mass. That means the random Dirac mass creates spontaneously a contribution which would be expected from a random energy term. This fact indicates that an additional random energy term may not qualitatively change the properties of the random Dirac mass.

The average local DOS can now be directly calculated from Eq. (20) in SPA,

$$\langle \rho^{\alpha\alpha}(r, M) \rangle_{\delta M} \approx \frac{\eta}{\pi g} = \frac{1}{2\pi g} \sqrt{m_c^2 - m^2} \Theta(m_c^2 - m^2), \quad (23)$$

where $\Theta(x)$ is the Heaviside step function. We see that a semicircle law is reproduced. In the following we will consider only the regime where the average local DOS is non-zero, i.e., $m^2 < m_c^2$.

B. Gaussian fluctuations

In order to evaluate the second moment of the local DOS the Gaussian fluctuations around the SP must be calculated. Since Q , P , and Θ are 2×2 matrices, the fluctuations can also be parametrized as four-component vector fields: $q_1 = \delta Q_{11}$, $q_2 = (\delta Q_{12} + \delta Q_{21})/2$, $q_3 = -i(\delta Q_{12} - \delta Q_{21})/2$, $q_4 = \delta Q_{22}$ with analogous definitions for p_1, \dots, p_4 and the Grassmann field ψ_1, \dots, ψ_4 with $\psi_2 = (\Theta_{12} + \Theta_{21})/2$ and $\psi_3 = -i(\Theta_{12} - \Theta_{21})/2$. The action of the Gaussian fluctuations reads, in Fourier representation²⁰

$$S \approx \int \sum_{\mu, \mu'=1}^4 (\mathbf{I}_k)_{\mu, \mu'} (q_{k, \mu} q_{-k, \mu'} + p_{k, \mu} p_{-k, \mu'} + 2\psi_{k, \mu} \psi_{-k, \mu'}) d^2k, \quad (24)$$

with the fluctuation matrix \mathbf{I}_k . The stability matrix reads

$$\mathbf{I}(k') = \begin{pmatrix} I_{11} & I_{12} & I_{13} & I_{14} \\ -I_{12}^*/\rho & I_{22} & I_{23} & \rho I_{12} \\ -I_{13}^*/\rho & I_{23} & I_{33} & \rho I_{13} \\ I_{14}^* & -I_{12}^* & -I_{13}^* & I_{11}^* \end{pmatrix}, \quad (25)$$

with $\rho = \mu/\mu^*$ and $\mu = m/2 + i\eta$. In particular, for a vanishing wave vector we have

$$\mathbf{I}(k'=0) = \begin{pmatrix} 1/g - \mu^{*2}/2\pi|\mu|^2 & 0 & 0 & 1/g - 1/2\pi \\ 0 & 2/g - 1/\pi & 0 & 0 \\ 0 & 0 & 2/g - 1/\pi & 0 \\ 1/g - 1/2\pi & 0 & 0 & 1/g - \mu^2/2\pi|\mu|^2 \end{pmatrix}. \quad (26)$$

Thus the Gaussian fluctuations are always massive except for the critical points $m = \pm m_c$. This reflects the discrete symmetry of the Hamiltonian (4) (for a more detailed discussion of the symmetry properties see Ref. 20). For $k' \sim 0$ we obtain

$$I_{11} = 1/g - \mu^{*2}/2\pi|\mu|^2, \quad I_{12} = \frac{\mu^*}{2\pi|\mu|} \frac{k_2'}{|\mu|}, \quad I_{13} = \frac{\mu^*}{2\pi|\mu|} \frac{k_1'}{|\mu|}, \\ I_{14} = 1/g - 1/2\pi + o(k'^2), \quad I_{23} = \frac{1}{2\pi} \frac{k_1' k_2'}{|\mu|^2}, \quad I_{22/33} = 2/g - 1/\pi, \quad (27)$$

that is, I_{14} is real.

C. Expansion of \mathcal{G}

Retaining only terms up to the second order, we have

$$\langle \mathcal{G}_{12, kj} \mathcal{G}_{21, jk} \delta_{\alpha, \beta} - \mathcal{G}_{11, jj} \mathcal{G}_{22, kk} \rangle_Q + \langle \mathcal{G}_{11, jj} \rangle_Q \langle \mathcal{G}_{11, kk} \rangle_Q \approx 4 \delta_{\alpha, \beta} \langle [\mathcal{G}_0 \tau \Theta \tau \mathcal{G}_0]_{rr, kj} [\mathcal{G}_0 \tau \Theta \tau \mathcal{G}_0]_{rr, jk} \rangle_{\delta Q}, \quad (28)$$

with

$$\mathcal{G}_0 = \begin{pmatrix} (H_0 - 2\tau Q_0 \tau + i\omega \sigma_0)^{-1} & 0 \\ 0 & (H_0 - 2\tau Q_0 \tau + i\omega \sigma_0)^{-1} \end{pmatrix}. \quad (29)$$

Now we have to perform the Grassmann integrations, ending up with

$$\langle \Theta_{j'j'',r'} \mathcal{G}_{k'k'',r''} \rangle_{\delta Q} = U_{j'j'',v} U_{k'k'',v'}^T \langle \psi_{v,r'} \mathcal{G}_{v',r''} \rangle_{\delta Q} = (1/2) U_{j'j'',v} U_{k'k'',v'}^T \mathbf{I}_{r'',vv'}^{-1}, \quad (30)$$

with the unitary matrix

$$U = \frac{1}{\sqrt{2}} \begin{pmatrix} 1 & 0 & 0 & 0 \\ 0 & 1 & -i & 0 \\ 0 & 1 & i & 0 \\ 0 & 0 & 0 & 1 \end{pmatrix}. \quad (31)$$

The stability matrix (26) has one zero eigenvalue if μ is real, i.e., for $m = \pm m_c$. Consequently, there is a singularity in the Fourier components of $\mathbf{I}(k)$ at $k=0$. The leading behavior in the $k \sim 0$ asymptotics of \mathbf{I}^{-1} can be extracted as

$$\begin{pmatrix} \langle \Theta_{11} \mathcal{G}_{11} \rangle_{\delta Q} & \langle \Theta_{11} \mathcal{G}_{22} \rangle_{\delta Q} \\ \langle \Theta_{22} \mathcal{G}_{11} \rangle_{\delta Q} & \langle \Theta_{22} \mathcal{G}_{22} \rangle_{\delta Q} \end{pmatrix} = \frac{1}{2} \begin{pmatrix} \mathbf{I}_{11}^{-1} & \mathbf{I}_{14}^{-1} \\ \mathbf{I}_{41}^{-1} & \mathbf{I}_{44}^{-1} \end{pmatrix} = \frac{-1/4}{1 - \cos(2x) + (g/2\pi|\mu|^2)\cos(x)k^2} \begin{pmatrix} -2\pi + e^{2ix}g & 2\pi - g \\ 2\pi - g & -2\pi + e^{-2ix}g \end{pmatrix}, \quad (32)$$

where $\mu^* = |\mu|e^{ix}$. We consider weak fluctuations: higher order contributions in g in the numerator and in the coefficient of k^2 have been neglected. We make use of the following approximation

$$\begin{aligned} (H_0 - 2\tau Q_0 \tau + i\omega \sigma_0)_{rr'}^{-1} &\approx \delta_{r,r'} \int (|\mu|^2 + k^2)^{-1} \\ &\times d^2k / (2\pi)^2 \begin{pmatrix} \mu^* & 0 \\ 0 & -\mu \end{pmatrix} \\ &= (1/4\pi) \delta_{r,r'} \ln(1 + \lambda^2 |\mu|^{-2}) \\ &\times \begin{pmatrix} \mu^* & 0 \\ 0 & -\mu \end{pmatrix}, \quad (33) \end{aligned}$$

where λ is a UV cutoff. For simplicity, we assume in the following $\lambda = 1$. Then the second moment of the local DOS reads

$$M_2^{\alpha\beta} = \delta_{\alpha\beta} \pi^{-2} \sum_{l,l'} \gamma_l^2 \gamma_{l'}^2 \tau_l^2 \tau_{l'}^2 \int K_{l,l'}(k) d^2k / (2\pi)^2, \quad (34)$$

with $K_{1,1} = \mathbf{I}_{11}^{-1}$, $K_{1,2} = \mathbf{I}_{14}^{-1}$, $K_{2,1} = \mathbf{I}_{41}^{-1}$, and $K_{2,2} = \mathbf{I}_{44}^{-1}$, and $\gamma_1 = \mu^* \ln(1 + |\mu|^{-2})$, $\gamma_2 = -\gamma_1^*$. Furthermore,

$$\begin{aligned} M_2^{\alpha\beta} &= \delta_{\alpha,\beta} \pi^{-2} [2\text{Re} \mu^{*4} (2\pi - e^{2ix}g) \\ &- 2|\mu|^4 (-2\pi + g)] C \int \{1 - \cos(2x) \\ &+ [g \cos(x)/2\pi |\mu|^2] k^2\}^{-1} \\ &\times d^2k / (2\pi)^2, \quad (35) \end{aligned}$$

where $C = [(1/4\pi) \ln(1 + |\mu|^{-2})]^4 / 2$. The factor in front of the integral reads also

$$\pi^{-2} \{4\pi [\cos(4x) + 1] - 2g [\cos(2x) + 1]\} |\mu|^4. \quad (36)$$

Integration with respect to k gives

$$\begin{aligned} &\int \{1 - \cos(2x) + [g \cos(x)/2\pi |\mu|^2] k^2\}^{-1} k dk / 2\pi \\ &\sim -\frac{|\mu|^2}{2g \cos(x)} \ln \left\{ \frac{1 - \cos(2x)}{1 - \cos(2x) + [g \cos(x)/2\pi |\mu|^2]} \right\}. \quad (37) \end{aligned}$$

Then

$$\begin{aligned} M_2^{\alpha\beta} &\approx -\delta_{\alpha,\beta} C \frac{4|\mu|^6 [\cos(4x) + 1]}{g \cos(x)} \\ &\times \ln \left\{ \frac{1 - \cos(2x)}{1 - \cos(2x) + [g \cos(x)/2\pi |\mu|^2]} \right\}. \quad (38) \end{aligned}$$

IV. DISCUSSION

Making use of the evaluation described above, we can now display and discuss the dependence of M_2 on the effective chemical potential $m = \mu - t'$ and on the amount of chaos or disorder in each single dot, g . According to the average DOS (23) there is a narrow band of bulk electronic states. Moreover, there are also edge states which carry the Hall current for $m > m_c$. In the following we will discuss only the bulk states. At the band center the second moment of the LDOS is $M_2^{\alpha\beta} = \delta_{\alpha\beta} (m_c/2g)^4 / \pi$. The ratio $\sqrt{M_2}/\rho$ at $m=0$ then is $\sqrt{\pi} m_c/2g$.

Figure 1 shows the dependence of M_2 (suitably scaled) on the parameters m and g . This figure, obtained for typical values of the parameters, displays an interesting dramatic increase as a function of m for the second moment M_2 of the local DOS as the edge of the energy band, $m = m_c$, is approached. This (logarithmic) divergence of M_2 at the edge of the band indicates a power law singularity for the fluctuations near the QHT. This is in agreement with the results of

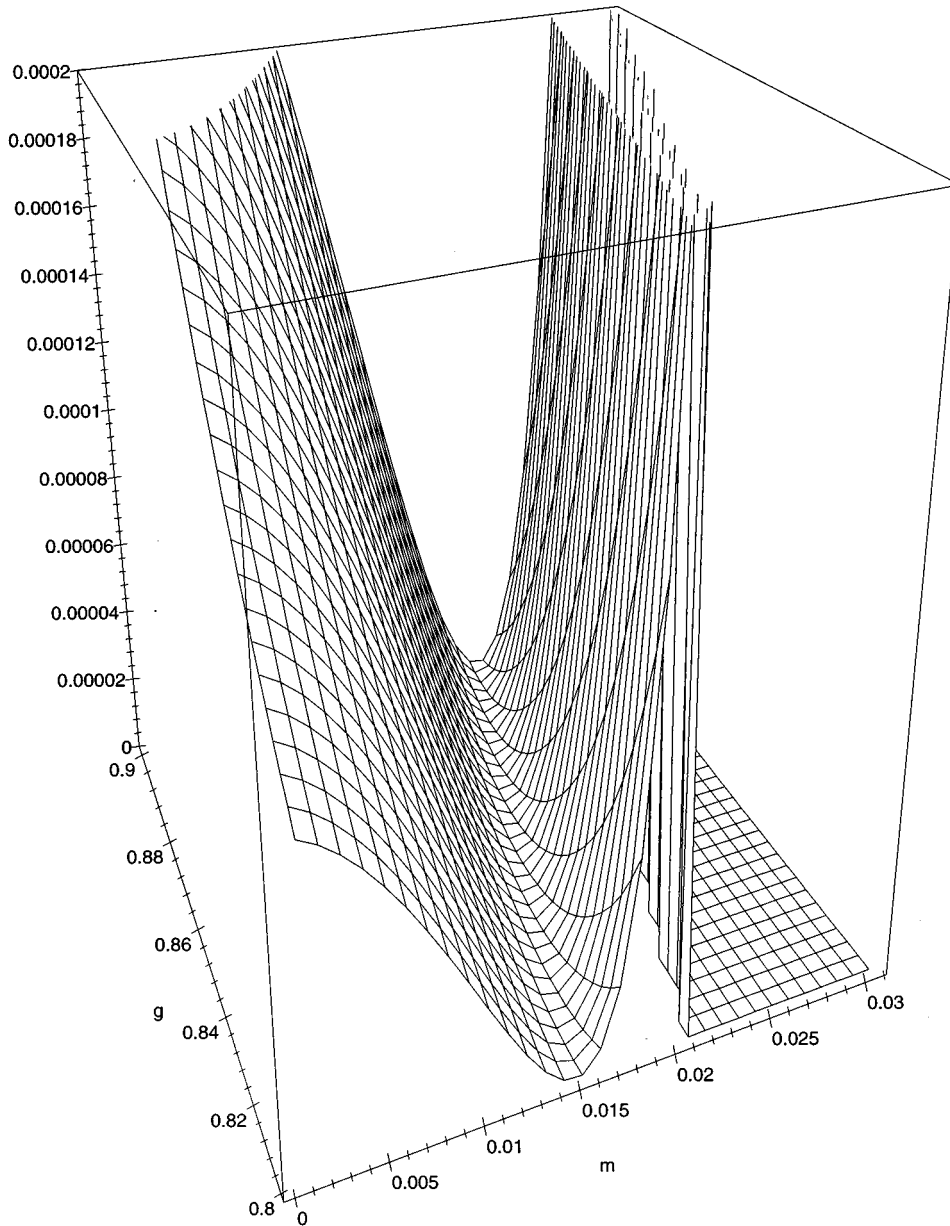


FIG. 1. Second moment M_2 of the local density of states (LDOS) as function of effective chemical potential m and strength of level fluctuations g .

the $2 + \epsilon$ expansion.^{23,24} Also, notice that, as they should, the fluctuations decrease as randomness decreases, except in the vicinity of $m = m_c$. To our knowledge, these results, obtained for a realistic lattice of "artificial atoms," have not been discussed before (but see, however, below). The data in Fig. 1 show quite clearly the presence of important fluctuations in the local DOS as a consequence of single-dot level fluctuations, the fluctuations becoming perhaps critical at the edge of the band.

The level fluctuations for an isolated quantum dot are described by a single random matrix $\sigma_3 M^{\alpha\beta}$ which remains from the Hamiltonian of Eq. (4). The random matrix has, in contrast to the full Hamiltonian (4), a continuous unitary symmetry. This generates in the $N \rightarrow \infty$ limit a saddle-point manifold which we have to integrate out. The remaining functional is a zero-dimensional nonlinear σ model²⁸ for the evaluation of the fluctuations of the DOS. The crossover from the fully coupled quantum dots to isolated dots can be achieved by decreasing the tunneling rates t and t' . Since t was scaled out in the Hamiltonian, we must study for

this purpose the rescaled mass m/t and the rescaled disorder parameter g/t^2 . Sending $t \rightarrow 0$, m_c goes like $2t/\sqrt{\exp(2\pi^2/g) - 1} \rightarrow \sqrt{2g/\pi}$. Therefore, the level fluctuations create a broad "band" which is suppressed by the tunneling term to a much narrower band. Moreover, the fluctuations of the local DOS are also reduced by the tunneling between the quantum dots.

Notice that the strength of the fluctuations in the local DOS depends on the parameter $m = \mu - t'$. This requires tuning the value of the chemical potential μ or of the next-neighbor hopping t' . Both could be achieved in experimentally realizable QDA by means of a varying gate voltage or a suitable design in the gate structure and in its voltages.

It is important to discuss, at this point, the relevance of our calculation for perspective experimental observations on QDA. To our knowledge the local DOS can be accessed experimentally by two possibilities: the Knight shift of the NMR (nuclear magnetic resonance) line shape due to the electron polarization²⁵ and the SET (single-electron tunneling) technique.¹¹ From these measurements one can gain ac-

cess to the statistics of the local DOS mesoscopic fluctuations.

A. NMR Knight shift spectroscopy

We begin by discussing the NMR Knight shift technique, which has recently witnessed considerable revival both for mesoscopic semiconductor structures and for high-temperature superconductors. For zero-dimensional mesoscopic structures (single dots, small metallic particles, or random aggregates of these) the Knight shift method has been discussed by Efetov and Prigodin^{19,26} and by Fal'ko and Efetov.²⁷ For the one-dimensional disordered metal a related discussion for the connection between the local DOS and the Knight shift can be found in the work of Altshuler and Prigodin.²⁸ Here we give a formulation for the Knight shift in a 2D QDA. We adapt the treatment for the Knight shift in a traditional solid (like, e.g., Li) (Ref. 25) to the situation in which a (2D) solid of "artificial atoms" is considered. Assume that a tight-binding description of quasielectron tunneling (or hopping) is appropriate (as advocated in the calculation of the previous sections) and that a single-dot confining potential approximately of the square-well type can be used to describe the single "atomic" levels $\{E_\alpha, \varphi_\alpha(\mathbf{r})\}$ of a single dot. Then a "band-structure" approach becomes a realistic calculation of the energy levels of the entire 2D QDA made up of these "atoms" and we can envisage the creation of "bands" of energy states from each "atomic" level E_α . We label the 2D QDA energy levels, therefore, $E_\alpha(\mathbf{k}) = E_\alpha + \sum_\delta e^{i\mathbf{k}\cdot\boldsymbol{\delta}}$ and these will normally overlap due to the closeness of the levels E_α of the single dots. By building the many-electron wave function in the normal way, the hyperfine interaction Hamiltonian can be averaged over the electronic degrees of freedom to give the contribution to the nuclear Hamiltonian arising from the electron polarization in the QDA that ultimately leads to the Knight shift formula,

$$\frac{\Delta\omega(\mathbf{r})}{\omega_0} = \frac{8\pi}{3} \int d\varepsilon \chi(\varepsilon) \rho(\mathbf{r}, \varepsilon) \langle |u_\varepsilon(\mathbf{r})|^2 \rangle_{E_\alpha(\mathbf{k})=\varepsilon}, \quad (39)$$

at the nuclear site \mathbf{r} . In the above formula, beside the local DOS which is the subject of the present investigation, appear also the single dot wave function $u_\varepsilon(\mathbf{r})$ (averaged over an equal-energy surface) and the electron spin susceptibility

$$\begin{aligned} \chi(\varepsilon) &= \frac{1}{H_0} \gamma_e \hbar^{\frac{1}{2}} (f(\varepsilon, -\frac{1}{2}) - f(\varepsilon, \frac{1}{2})) \\ &\approx \frac{(\gamma_e \hbar)^2}{8k_B T} \frac{1}{\cosh^2\left(\frac{\varepsilon - E_F}{k_B T}\right)}, \end{aligned} \quad (40)$$

where the approximation holds at low temperatures [where the Fermi distribution function $f(\varepsilon, m_s)$ can be expanded]. Since the low-temperature form of $\chi(\varepsilon)$ is δ -like, we essentially get that the Knight shift is proportional to the local DOS, evaluated at the Fermi level, however through a multiplicative constant that is in principle also randomly distributed, in a way that is beyond the scope of the present treatment. We conclude with the form

$$\frac{\Delta\omega(\mathbf{r})}{\omega_0} \approx \frac{8\pi}{3} \langle |u_\varepsilon(\mathbf{r})|^2 \rangle_{\varepsilon=E_F} \chi(E_F) \rho(E_F, \mathbf{r}), \quad (41)$$

for the expected Knight shift from a QDA. If we assume that the wave function at the Fermi level has much smaller fluctuations than the local DOS, then the moments of the local DOS can be extracted by looking at the moments of the Knight shift itself.

B. Single-electron tunneling spectroscopy

SET spectroscopy is well known as a tool for the investigation of discrete single- and few-electron energy states in quantum dots.²⁹ Lerner and Raikh³⁰ have proposed to apply the technique to study the weak-localization effects in disordered heterostructures, and the use of SET spectroscopy for imaging the local DOS in a disordered (bulk) semiconductor heterostructure has been recently reported.¹¹ Thus, SET spectroscopy appears to be a promising tool for an experimental investigation of local DOS fluctuations in a QDA.

Lerner and Raikh³⁰ show that, for the resonant-tunneling junction geometry, the measurement of the conductance G_t gives direct imaging of the local DOS, ρ :

$$G_t = \frac{\pi e^2 S \Gamma_0}{2k\hbar} \rho, \quad (42)$$

with Γ_0 , k , and S geometrical parameters. A more complicated treatment ensues for a disordered material in the junction's barrier. The conductance presents mesoscopic fluctuations at low temperatures and one can show³⁰ that the second moments of local DOS and conductance are related by the formula

$$\frac{M_2(G_t)}{\langle G_t \rangle} \propto \frac{M_2(\rho)}{\langle \rho \rangle}. \quad (43)$$

However, Schmidt *et al.*¹¹ propose a double-barrier tunneling experimental geometry which leads through the measurement of the I - V characteristic to the relation

$$\delta G(\mathbf{r}) = \delta(dI/dV) \propto \delta(d\rho(\mathbf{r}, E)/dE), \quad (44)$$

for the local fluctuations of the conductance G of the disordered sample. Thus, SET spectroscopy can provide information, in principle, to local DOS statistical properties perhaps also in the case of a QDA setup.

We mention, before concluding this subsection, the possibility of imaging the local DOS for surface electronic states also by means of scanning-tunneling microscopy.³¹ This technique also relies on the measurement of the differential conductance, dI/dV , at local sample's sites; from this, the shape of the local DOS and its fluctuations' statistics can be reconstructed. This technique is perhaps more suitable for 2D systems like our QDA.

Whether from the Knight shift in NMR or from the conductance in SET experiments, the measurement of the value of the local DOS in a real QDA should allow (via, e.g., repeated measurements) for a statistics of its fluctuations and the experimental determination of M_2 . This will be an indirect observation of the existence of level fluctuations in single quantum dots.

C. Beyond 2D: $d=2+\epsilon$, 1 and 0 dimensions

In dimensions higher than $d=2$, there already exist calculations of the second moment of the local DOS for the situation in which randomness creates a mobility edge in the Anderson transition for a disordered metal.³² These calculations are based on $2+\epsilon$ -type expansions on the Q -matrix nonlinear σ model and lead to the result that $M_2 \sim (E - E_C)^{-\mu_2}$ with $\mu_2 = 2 + O(\epsilon)$. This shows the existence of the possibility of a divergence for the second moment of the local DOS near the mobility edge. Although the Anderson transition situation is not exactly the same QDA problem treated in the present paper, nevertheless these calculations show that a divergence of M_2 is to be expected.

In lower dimensions, we recall the work of Altshuler and Prigodin, for $d=1$,²⁸ and of Efetov and Prigodin, for $d=0$ (Ref. 26) (a single dot in our picture), for the case of a disordered metal. In $d=1$, exact diagrammatic techniques can be employed to work out the entire probability distribution for the local DOS of a weakly disordered metal. The resulting distribution depends strongly on the type (open or closed) of boundary conditions. Finally, in $d=0$ the nonlinear- σ -model calculations involving supersymmetry of Refs. 19,26 can be employed.

D. Conclusions

We have shown how, by means of the technique of Dirac fermions in $d=2$, one can characterize the distribution of the fluctuations of the local DOS in the proximity of an IQHE transition. We have restricted the calculation to characterize the second moment $M_2(\rho)$, but in principle also the higher moments can be evaluated (with increasing technical difficulties).

We have made extensive use of the fact that in the Dirac fermions approach one is dealing with a unique saddle-point solution, unlike in the case of the nonlinear- σ -model approach. This is a consequence of the discrete symmetry of the model of Ludwig *et al.*⁷ for the case of a random mass, which we use for our calculations. This simple structure of the saddle-point solution made the 2D calculation possible.

ACKNOWLEDGMENTS

This work was supported in part (G.J.) by EC Contract No. ERB4001GT957255.

*On leave from: Istituto di Scienze Matematiche, Fisiche e Chimiche, Università di Milano a Como, Via Lucini 3, 22100 Como, Italy (permanent address).

¹*Mesoscopic Phenomena in Solids*, edited by B. L. Altshuler, P. A. Lee, and R. A. Webb, Modern Problems in Condensed Matter Sciences Vol. 30 (North-Holland, Amsterdam, 1991).

²*Quantum Dynamics of Submicron Structures*, Vol. E291 of *NATO Advanced Study Institute, Series B: Physics*, edited by H. A. Cerdeira, B. Kramer, and G. Schön (Kluwer, Dordrecht, 1995).

³D. Weiss, *Elektronen in "künstlichen" Kristallen* (Verlag Harri Deutsch, Frankfurt, 1994); D. Weiss, K. Richter, A. Menschig, R. Bergmann, H. Schweizer, K. von Klitzing, and G. Weimann, *Phys. Rev. Lett.* **70**, 4118 (1993).

⁴K. von Klitzing, G. Dorda, and M. Pepper, *Phys. Rev. Lett.* **45**, 494 (1980).

⁵B. I. Halperin, *Phys. Rev. B* **25**, 2185 (1982).

⁶*The Quantum Hall Effect*, 2nd ed., edited by R. E. Prange and S. M. Girving (Springer-Verlag, New York, 1990); M. Januën, O. Viehweger, U. Fastenrath, and J. Hajdu, *Introduction to the Theory of the Integer Quantum Hall Effect* (VCH Verlagsgesellschaft, Weinheim, 1994); T. Chakraborty and P. Pietiläinen, *The Quantum Hall Effects*, 2nd ed. (Springer-Verlag, Berlin, 1995).

⁷A. W. W. Ludwig, M. P. A. Fisher, R. Shankar, and G. Grinstein, *Phys. Rev. B* **50**, 7526 (1994); see also, M. P. A. Fisher and E. Fradkin, *Nucl. Phys. B* **251**, 457 (1985).

⁸K. Ziegler, *Europhys. Lett.* **28**, 49 (1994).

⁹K. Ziegler, *Phys. Rev. B* **55**, 10 602 (1997).

¹⁰S. E. Barrett, G. Dabbagh, L. N. Pfeiffer, K. W. West, and R. Tycko, *Phys. Rev. Lett.* **74**, 5112 (1995).

¹¹T. Schmidt *et al.*, *Europhys. Lett.* **36**, 61 (1996); *Solid-State Electron.* **40**, 15 (1996).

¹²F. Wegner, *Z. Phys. B* **35**, 207 (1979); **36**, 209 (1980).

¹³L. Schäfer and F. Wegner, *Z. Phys. B* **38**, 113 (1980); A. M. M. Pruisken and L. Schäfer, *Nucl. Phys. B* **200**, 20 (1982).

¹⁴D. H. Cobden and E. Kogan, *Phys. Rev. B* **54**, 17 316 (1996).

¹⁵Z. Wang, B. Jovanović, and D.-H. Lee, *Phys. Rev. Lett.* **77**, 4426 (1996).

¹⁶S. Cho and M. P. A. Fisher, *Phys. Rev. B* **55**, 1637 (1997).

¹⁷E. P. Wigner, *Ann. Math.* **53**, 36 (1951); **67**, 325 (1958).

¹⁸M. L. Mehta, *Random Matrices* (Academic Press, New York, 1967).

¹⁹K. B. Efetov, *Adv. Phys.* **32**, 53 (1983); *Supersymmetry in Disordered Systems and Chaos* (Cambridge University Press, Cambridge, 1997).

²⁰K. Ziegler, *Nucl. Phys. B* **344**, 499 (1990).

²¹E. Fradkin, *Phys. Rev. B* **33**, 3257 (1986); **33**, 3263 (1986).

²²A. Glimm and A. Jaffe, *Quantum Physics* (Springer Verlag, New York, 1981).

²³F. Wegner, *Z. Phys. B* **36**, 209 (1980).

²⁴A. M. M. Pruisken, *Phys. Rev. B* **32**, 2636 (1985).

²⁵G. P. Slichter, *Principles of Magnetic Resonance*, Springer Series in Solid State Science Vol. 1 (Springer, Berlin 1980).

²⁶K. B. Efetov and V. N. Prigodin, *Phys. Rev. Lett.* **70**, 1315 (1993); *Mod. Phys. Lett. B* **7**, 981 (1993).

²⁷V. I. Fal'ko and K. B. Efetov, *Phys. Rev. B* **50**, 11 267 (1994).

²⁸B. L. Altshuler and V. N. Prigodin, *Zh. Eksp. Teor. Fiz.* **95**, 348 (1989) [*Sov. Phys. JETP* **68**, 198 (1989)].

²⁹R. C. Ashoori, *Nature (London)* **379**, 413 (1996).

³⁰I. V. Lerner and M. E. Raikh, *Phys. Rev. B* **45**, 14 036 (1996).

³¹M. F. Crommie, C. P. Lutz, and D. M. Eigler, *Nature (London)* **363**, 524 (1993); Y. Hasegawa and Ph. Avouris, *Phys. Rev. Lett.* **71**, 1071 (1993).

³²F. Wegner, *Z. Phys. B* **36**, 209 (1980).